CHAPTER IV

PREPARATION AND CHARACTERIZATION OF GRAPHENE OXIDE / YTTRIUM OXIDE NANOCOMPOSITES FOR DYE SENSITIZED SOLAR CELL APPLICATIONS

4.1 INTRODUCTION

The rapidly growing application for global energy has significantly promoted the development of photovoltaic technologies, which can convert clean and renewable solar energy into electrical energy [1]. Dye sensitized solar cells with natural dyes as sensitizer are pollution free and have simple fabrication procedures that have received great attention as an alternative to silicon – based DSSCs and synthetic dye solar cells. Among dye sensitized solar cell, counter electrode plays an important role in collection of electrons. Pt electrode is commonly used as a counter electrode for DSSCs but this high cost is main blockage for its use as a counter electrode in DSSCs. Graphene is a two-dimensional layer of carbon atoms with a hexagonal packed structure that is the newest member of the nano-carbon family [2]. Graphene-based nanocomposites show promise for a variety of potential applications, such as sensors, batteries, aerogel devices, supercapacitor, and solar cells.

Yttrium (yttria) oxide is one of the most stable metals and is white in colour. Yttrium oxide is one of the material for energy storage applications due to its chemical stability and good corrosion resistance. Hence, an attempt is being made to use graphene oxide/ yttrium oxide as a counter electrode material. The graphene oxide/yttrium oxide nanoparticles have high crystallinity and high phase purity. The calcination temperature also plays a vital role in improving the efficiency of the solar cell. Hence, this chapter focuses on the synthesis and characterization of graphene oxide/ yttrium oxide (5:1, 5:2, 5:3, 5:4 and 5:5) nanocomposites and these prepared nanocomposites can be used as counter electrode for dye sensitized solar cells [3,4]

4.2 MATERIALS AND EXPERIMENTAL

4.2.1 Materials

Graphene oxide is prepared using modified Hummers' method. Sodium hydroxide (NaOH), yttrium hydroxide ($Y(OH)_3$), yttrium oxide (Y_2O_3) are purchased from Sigma Aldrich and are used without further purification.

4.2.2 Preparation of Yttrium Oxide nanocomposites

Yttrium oxide (Y_2O_3) is prepared by using chemical precipitation method. To synthesize Y_2O_3 nanocomposites, 1.5 g of yttrium nitrate are dispersed in 10 ml of distilled water and are kept under sonication for 1 hour at room temperature. Consequently, NaOH (0.3 M) is dissolved in 30 ml of distilled water and are added drop by drop into the solution until the pH reaches 13 and are stirred for 6 hours at 50°C [5]. The colloidal mixture of $Y(OH)_3$ (yttrium hydroxide) is centrifuged at 6000 rpm for 15 min and the precipitate is washed several times with deionized water until the pH of supernatant solution reached the value of 7. The precipitate is then dried at 80°C in air for 6 hours. The nanocomposites are annealed at 500°C for 3 hours in a muffle furnace to convert into the corresponding Y_2O_3 nanopowders [6].

4.2.3 Preparation of GO/Y_2O_3 nanocomposites

Graphene oxide (GO) are synthesized by modified Hummers method. Graphene oxide/Yttrium oxide (GO/Y_2O_3) nanocomposites are prepared by simple chemical precipitation method by taking 100 mg of GO in 60 ml of distilled water and yttrium oxide into the dispersed solution and are stirred for 7 hours at 60°C. This homogenous solution is kept undisturbed for 12 hours at room temperature [7]. The precipitated water is separated and washed with distilled water and ethanol. The precursor is dried at 80°C to obtain the GO/Y_2O_3 nanocomposites.

4.2.4 Characterization Techniques

The crystalline structure of the prepared GO/NiO nanocomposites is studied by X-ray diffraction using X'PERT^3 Panalytica diffractometer system. The FT-IR spectra are recorded for the presence of the functional groups in the nanocomposites using Shimadzu IR affinity-1. The morphology and the microstructure of the samples

are studied using Field Emission scanning electron microscopy (FESEM) using a Hitachi S3000H microscope and high resolution transmission electron microscopy (HR-TEM) using Jeol JEM 2100.

4.3 RESULTS AND DISCUSSION

4.3.1 XRD Analysis

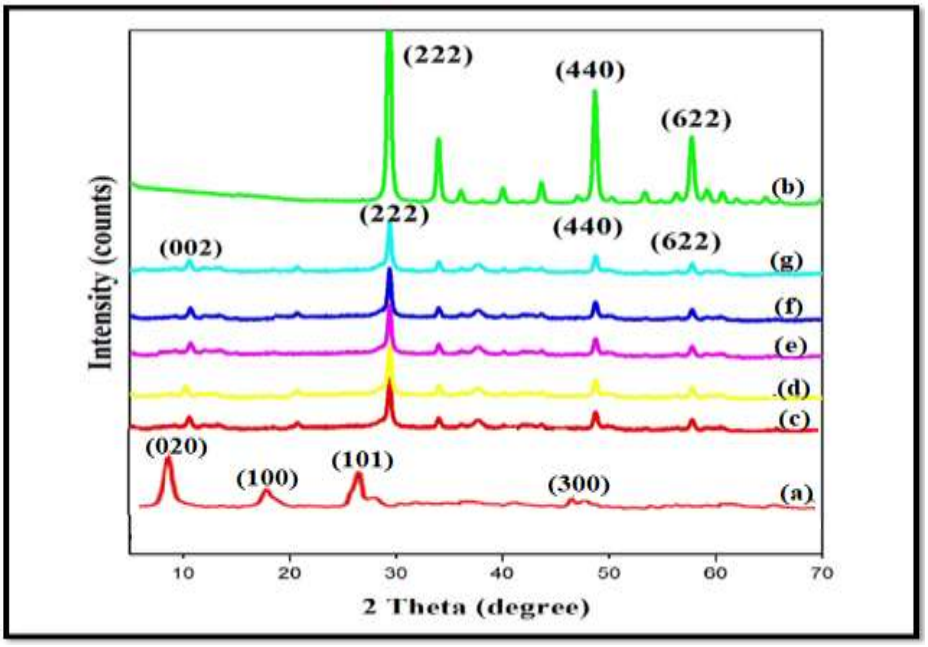

Figure 4.1 XRD images of (a) $Y(OH)_3$, (b) Y_2O_3 (c-g) GO/ Y_2O_3 (5:1, 5:2, 5:3, 5:4 and 5:5) nanocomposites

The XRD patterns of the prepared Y_2O_3 and GO/Y_2O_3 (5:1, 5:2, 5:3, 5:4 and 5:5) nanocomposites are shown in the Figure 4.1. The diffraction peaks of Y(OH)3 are observed at 2θ values of 9.38°, 19.5°, 30.01° and 51.2° corresponding to the (020), (100), (101) and (300) planes thereby confirming the formation of $Y(OH)_3$ as shown in the Figure. 4.1(a) [8]. The yttrium hydroxide is transformed into yttrium oxide by annealing the formed $Y(OH)_3$ at 700°C. It is observed from the Figure. 4.1(b) that the diffraction peaks at 2θ values of 10.01°, 20.06°, 29.03°, 48.05° and 57.06° are corresponding to the (020), (211), (222), (440) and (622) planes thereby confirming the formation of Y_2O_3, which is well matched with the JCPDS No. 24-1422. The average crystallite size for yttrium oxide is found to be around 19 nm [9]. The diffraction peaks appeared at 2θ values of 10.38°, 29.05°, 47.7° and 57.48°

correspond to the (002), (222), (440) and (622) planes of Y_2O_3 as shown in the Figure4.1(c-g) which confirms the formation of GO/Y_2O_3 nanocomposites. It is observed that on doping of Y_2O_3 into the GO, the intensity of Y_2O_3 peaks gets increased and the crystallite size is found to be around 23 nm. It is further observed that the intensity of the diffraction peaks corresponding to Y_2O_3 increases as the concentration increases from 5:1 to 5:5. The crystallite size of the prepared GO/Y_2O_3 (5:1, 5:2, 5:3, 5:4 and 5:5) nanocomposites are found to be 23 nm, 25.2 nm, 26.92 nm, 27.1 mm and 27.8 nm respectively [10]. The increase in the crystallite size may be due to the increase in the concentration of Y_2O_3 nanoparticles on the surface of Graphene oxide nanosheet. No impurity peaks are observed from XRD analysis and also further confirmed from EDAX analysis.

4.3.2 FTIR Spectral Analysis

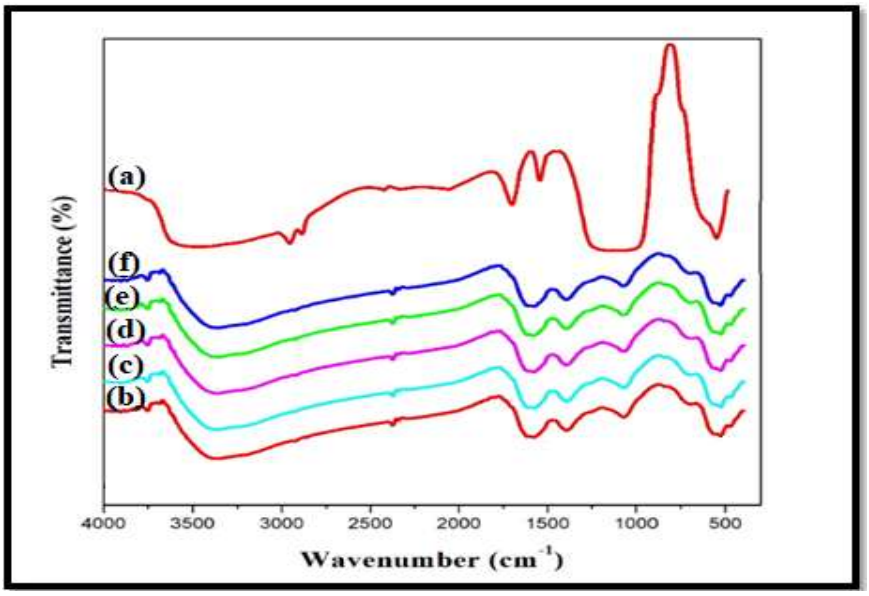

Figure 4.2(a-d) FT-IR spectra of (a) Y_2O_3 (b-f) GO/Y_2O_3 (5:1, 5:2, 5:3, 5:4 and 5:5) nanocomposites

FTIR measurement are employed to investigate the bonding interaction of prepared Y_2O_3 and GO/Y_2O_3nanocomosites. FT-IR spectra of the prepared yttrium oxide and GO/yttrium oxide (5:1, 5:2, 5:3, 5:4 and 5:5) nanocomposites are shown in the Figure 4.2 (a-f). The bands appeared at 615.1 cm^{-1} and 501 cm^{-1} are assigned to the stretching vibration of YO of Y_2O_3 nanocomposites as shows in the Figure 4.2 (a) It is observed from the Figure 4.2(b-f) that the yttrium oxide and GO nanocomposites

have similarity in their curve shape, and further a new band observed at 1505 cm^{-1} of GOY confirms that the Y_2O_3 has successfully composited with GO/Y_2O_3 (5:1, 5:2 5:3, 5:4 and 5:5). It is also observed from the Figure 4.2 (b-f) that the depth of the YO band at 501 cm^{-1} is gradually increased by increasing the concentration og Y_2O_3 from 5:1 to 5:5, which also confirms the Yttrium oxide nanoparticles are gradually spread on the surface of graphene oxide nanosheets. This results also confirmed from FESEM analysis [11,12].

4.3.3 Raman Spectroscopy

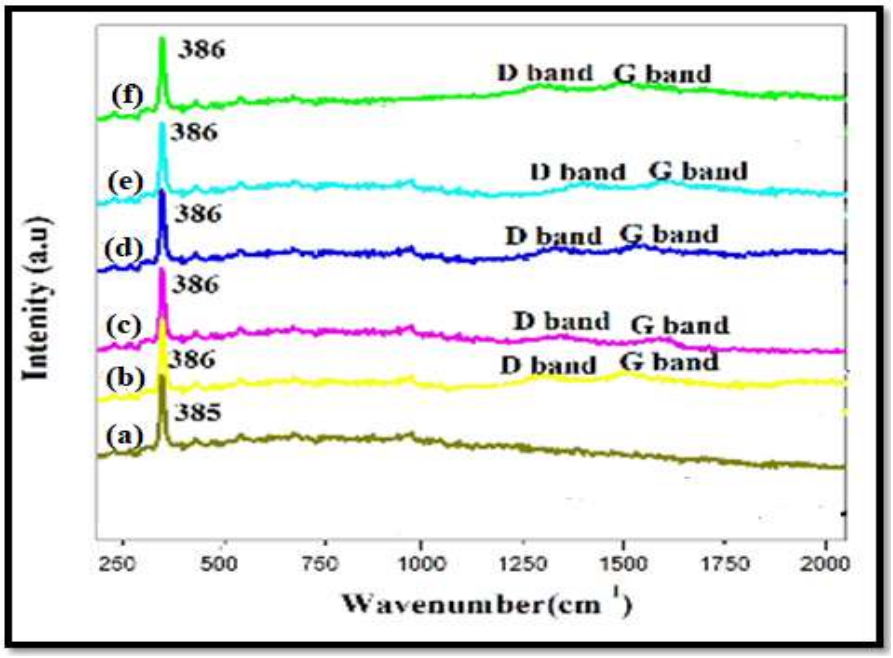

Figure 4.3 (a-e) Raman analysis of (a) Y_2O_3, (b-f) GO/ Y_2O_3 (5:1, 5:2, 5:3, 5:4 and 5:5) nanocomposites

Raman Spectroscopy is very useful to observe the structure and phase of materials. Figure 4.3 (a-e) shows that the Raman Scattering of GO, Y_2O_3 and GO/ Y_2O_3 (5:1, 5:2 5:3, 5:4 and 5:5) nanocomposites. The D band at 1352 cm^{-1} is due to structural disorders and defects, and the G band at 1594 cm^{-1} is corresponding to the sp^2 vibration of Graphene [13]. Figure 4.3 (b) shows that the intense band of the Y_2O_3 are located at 385 cm^{-1}. Figure 4.3 (c-e) shows three noticeable peaks at around 386 cm^{-1}, 1356 cm^{-1} and 1597 cm^{-1} which confirms the presence of GO and Y_2O_3 nanocomposites. The intensity of Yttrium oxide peak is increased and peaks are shifted. This may due to the increase in the concentration of Yttrium oxide on the surface of graphene oxide nanosheet.

4.3.4 FE-SEM

Surface morphology of the prepared nanocomposites are studied by Field emission electron microscope (FESEM). FESEM images of the prepared nanocomposites Y_2O_3, and GO/ Y_2O_3 (5:1, 5:2, 5:3, 5:4 and 5:5) are shows in the Figure 4.4 (a-f). Figure 4.4 (a) shows that the prepared Yttrium oxide nanoparticles has flake like structure. Figure 4.4 (b-f) showed that GO with different concentration of Y_2O_3 (5:1, 5:2, 5:3, 5:4 and 5:5) nanocomposites. It is observed that the number of Y_2O_3 nanoparticles on the surface of GO nanosheet is increased with increasing the concentration of Y_2O_3 nanoparticles [14,15]. Figure 4.4 (e) shows that the Graphene oxide nanosheet is rolled and this may due to the number of yttrium oxide nanoparticles on the surface of GO nanosheet. FESEM analysis confirmed that the Y_2O_3 nanoparticles are highly merged on the graphene oxide nanosheet.

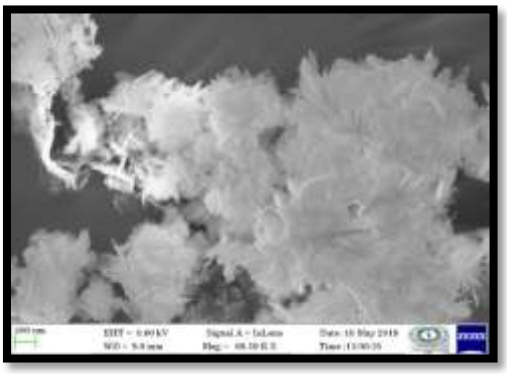

(a)

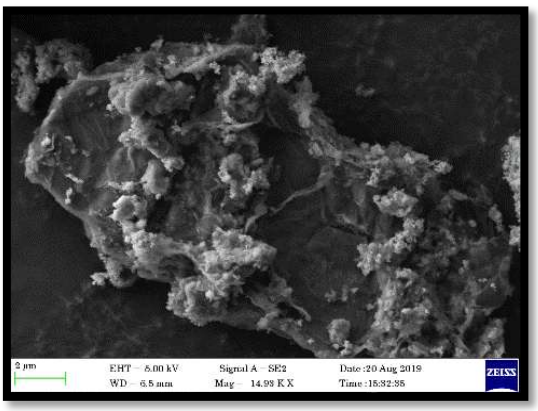

(b)

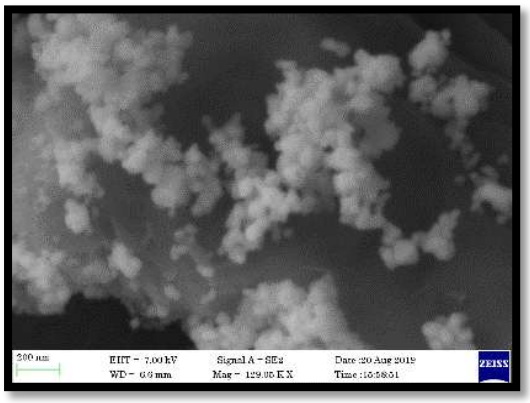

(c)

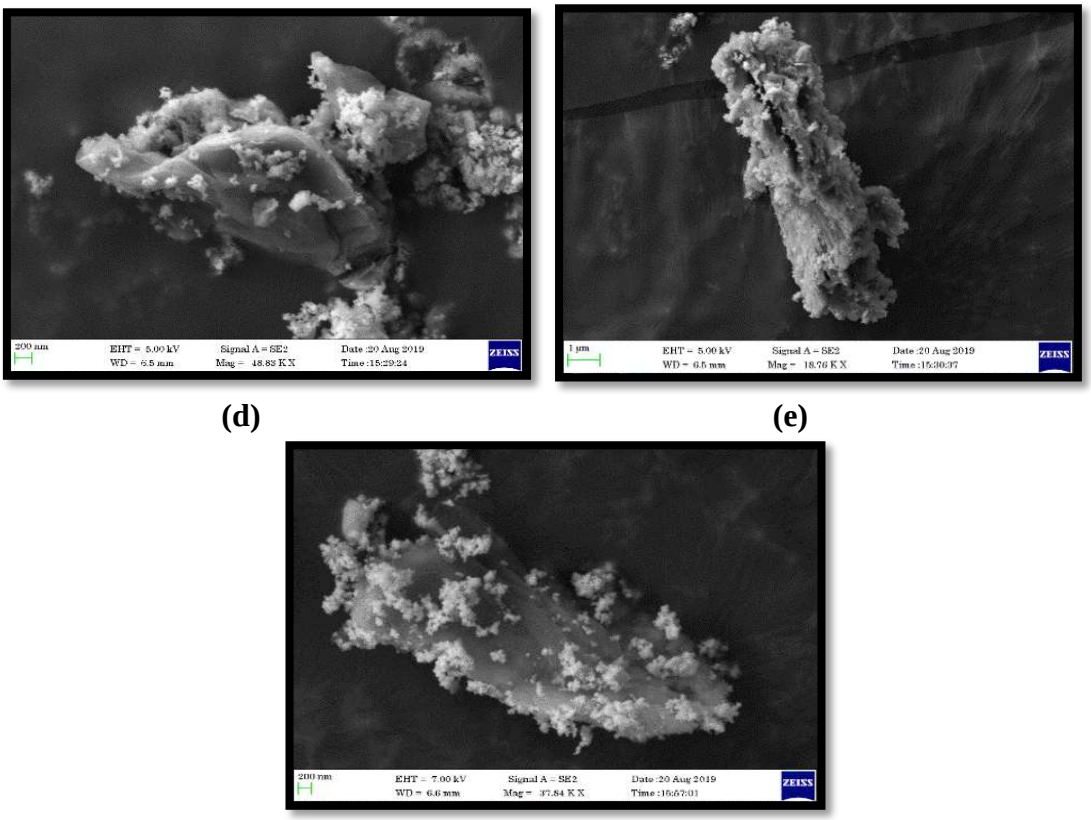

(d) **(e)**

(f)

Figure. 4.4 FESEM images of (a) Y_2O_3 (b-f) GO/Y_2O_3 (5:1, 5:2, 5:3, 5:4 and 5:5) nanocomposites

4.3.5 EDAX Analysis

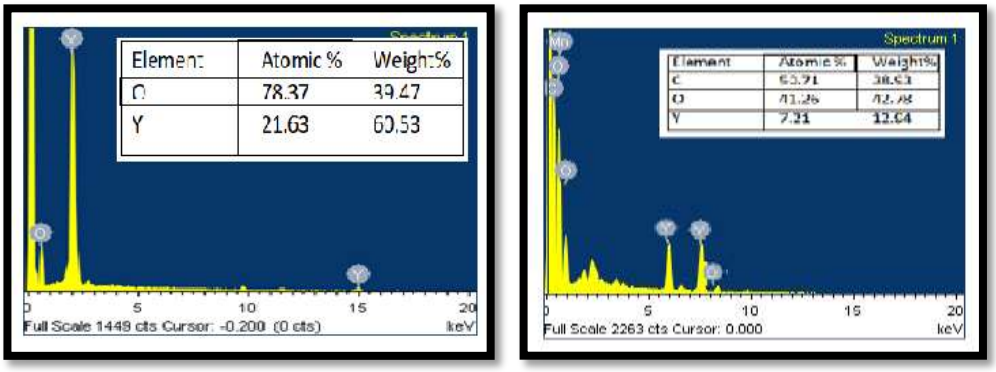

(a) **(b)**

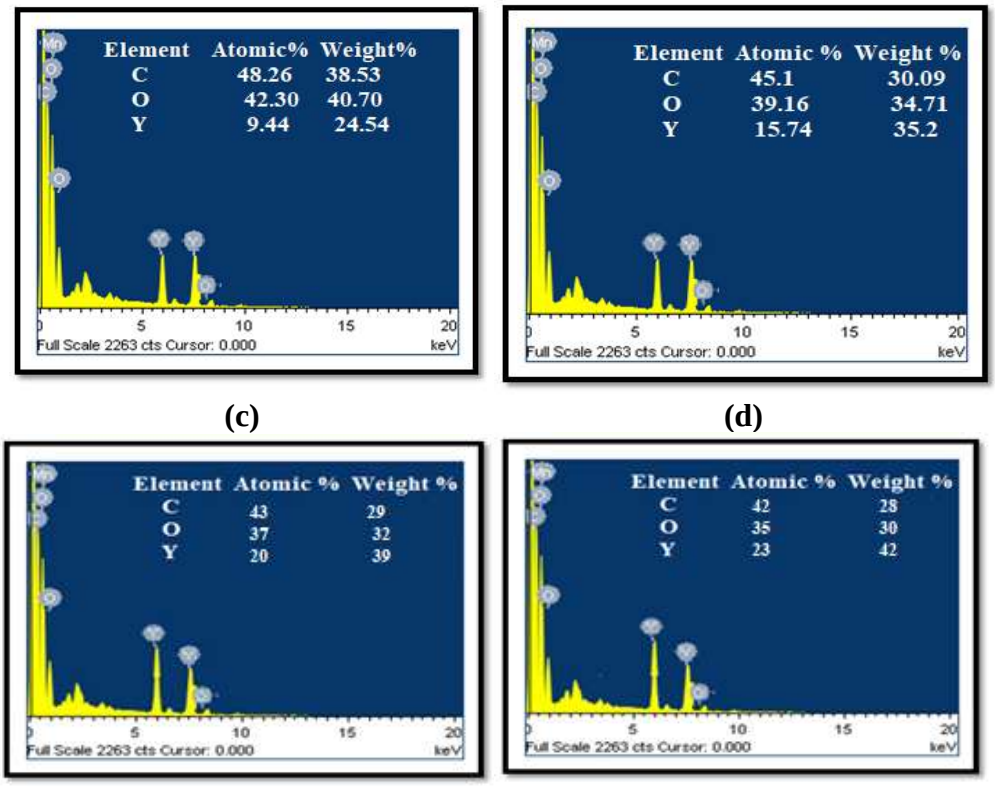

Figure 4.5 EDX spectra (a)Y_2O_3 (b-f) GO/Y_2O_3 (5:1, 5:2, 5:3, 5:4 and 5:5) nanocomposites

The Energy Dispersive Spectroscopy analysis is used to determine the percentage and composite formation of prepared nanocomposites. The EDX spectra of Y_2O_3 and GO/ Y_2O_3 (5:1, 5:2, 5:3, 5:4 and 5:5) nanocomposites are shown in the Figure 4.5 (a-f). Figure 4.5 (a) confirms the presence of Y and O elements without any impurities. Figure 4.5 (b-f) shows the presence of C, O and Y that confirms the formation of GO/Y_2O_3 (5:1, 5:2, 5:3, 5:4 and 5:5) with the atomic percentage and weight percentage are given as inset table. Atomic percentage of Yttrium in GO nanosheet (5:1, 5:2, 5:3, 5:4 and 5:5) concentrations are 7.21%, 9.44%, 15.74%, 20% and 23%respectively [16]. It is confirmed from EDAX analysis that with increase in the concentration of yttrium oxide from 5:1 to 5:5, the number of Yttrium nanoparticles on the Graphene oxide surface increases, which could also be evidenced from FESEM analysis.

4.3.6 HR-TEM Analysis

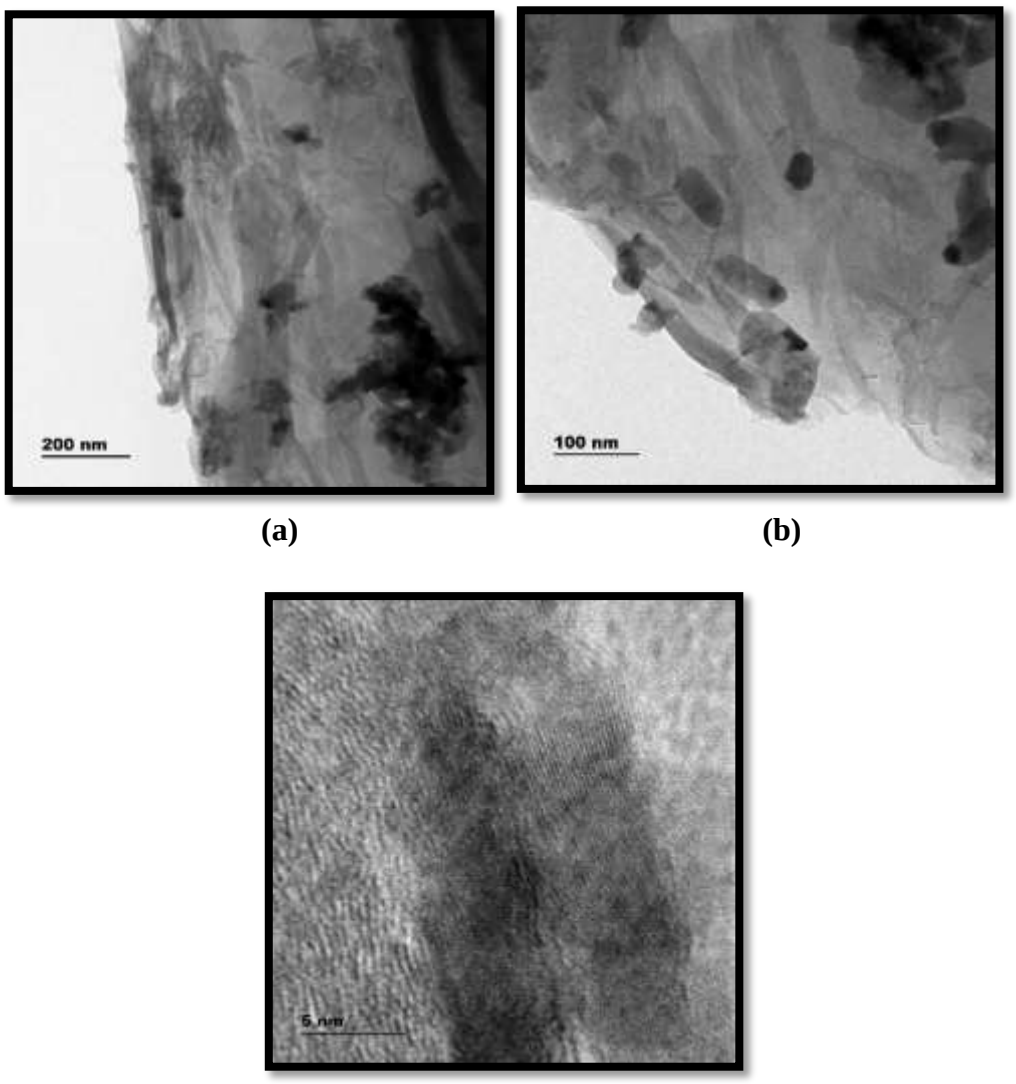

(a) **(b)**

(c)

Figure 4.6 (a-c) HRTEM images of GO / Y_2O_3(5:4) nanocomposites

Figure 4.6 (a-c) shows that the HR-TEM images of GO/Y_2O_3(5:4) nanocomposites. Figure 4.6 (a-c) shows that the flake like shape of Yttrrium oxide nanoparticles is gradually distributed on the surface of GO nanosheet. The distributed yttrium oxide nanoparticles are homogeneous without any impurities. This HR-TEM analysis confirms the formation of GO/Y_2O_3 nanocomposites [17].

4.3.7 Selected Area Electron Diffraction analysis

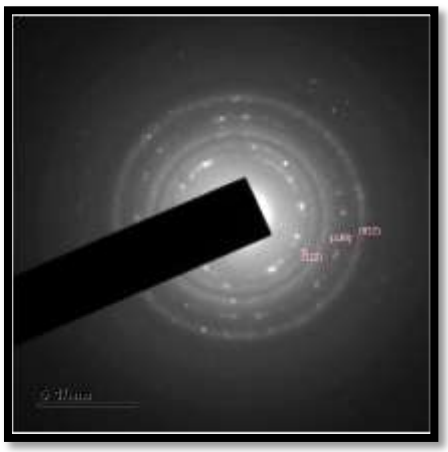

Figure 4.7 SAED image of Graphene oxide / Yttrium oxide (5:4) nanocomposites

The Selected area electron diffraction pattern (SAED) of the prepared nanocomposites GO/Y_2O_3 (5:4) is shows in the Figure 4.7. The SEAD results shows that the three discrete bright rings which indicates the successful formation of well crystalline natureY_2O_3nanoparticles on the surface of graphene oxide nanosheet [18]. Each rings corresponds to the (222), (440) and (622) planes of Yttrium oxide nanoparticles, which could also be corroborated by XRD analysis [19,20].

4.4 Conclusion

This chapter describes the Graphene oxide/ Yttrium oxide (5:1, 5:2, 5:3, 5:4 and 5:5) nanocomposites are synthesized by simple chemical precipitation method. The XRD analysis confirms the presence of GO/ Y_2O_3(5:1,5:2, 5:3, 5:4 and 5:5) nanocomposites and crystallite size is found to be 23 nm, 25.2 nm, 26.92 nm, 27.1 mm and 27.8 nm respectively. FESEM and HRTEM analysis confirms that the Yttrium oxide nanoparticles are evenly dispersed onto the surface of Graphene oxide nanosheet. EDAX analysis confirms the presence of Y, O and C elements without any impurities. The prepared nanocomposites can be used as a counter electrode for dye sensitized solar cell applications.

REFERENCES

1. S. Mathew, S. Aghazada, P. Comte, M. Gratzel, and M. K. Nazeeruddin, J. Mater. Chem. C 5, 2833 (2017).

2. B. Pashaei, H. Shahroosvand, and P. Abbasi, RSC Advances 5, 94814 (2015).

3. M.-N. H. Lirong Zhang, G. Sun, Y. Fan, G. Zhang, Y. Wang, and G. Lub, J. Chin. Chem. Soc 60, 1371 (2013).

4. F. Cao, G. Oskam, and P. C. Searson, The Journal of Physical Chemistry 99, 17071 (1995).

5. M.-S. Kang, J. H. Kim, J. Won, and Y. S. Kang, Journal of Photochemistry and Photobiology A: Chemistry 183, 15 (2006).

6. Z. Huo, S. Dai, K. Wang, F. Kong, C. Zhang, X. Pan, and X. Fang, Solar Energy Materials and Solar Cells 91, 1959 (2007).

7. M. Masamitsu, W. Yuji, K. Takayuki, S. Kouichiro, I. Teruhisa, I. Masaaki, and Y. Shozo, Bulletin of the Chemical Society of Japan 74, 387 (2001), https://doi.org/10.1246/bcsj.74.387 .

8. M. Parvez, I. In, J. Park, S. Lee, and S. Kim, Solar Energy Materials and Solar Cells 95, 318 (2011), 19th International Photovoltaic Science and Engineering Conference and Exhibition (PVSEC-19) Jeju, Korea, 9-13 November 2009.

9. O. Winther-Jensen, V. Armel, M. Forsyth, and D. R. MacFarlane, Macromolecular Rapid Communications 31, 479 (2010), https://onlinelibrary.wiley.com/doi/pdf/10.1002/marc.200900701 .

10. R. Komiya, L. Han, R. Yamanaka, A. Islam, and T. Mitate, Journal of Photochemistry and Photobiology A: Chemistry 164, 123 (2004), proceedings of the Dye Solar Cell Osaka ICP-21 Pre-symposium. Dedicated to Professor Shozo Yanagida on the occasion of his retirement.

11. O. A. Ileperuma, Materials Technology 28, 65 (2013), https://doi.org/ 10.1179/1753555712Y.0000000043 . 207 208

12. C. Wang, L. Wang, Y. Shi, H. Zhang, and T. Ma, Electrochimica Acta 91, 302 (2013).

13. L. Fan, S. Kang, J. Wu, S. Hao, Z. Lan, and J. Lin, Energy Sources, Part A: Recovery, Utilization, and Environmental Effects 32, 1559 (2010).

14. Y. H. Dai, X. L. Sun, Q. F. Shi, and M. S. Yang, in Renewable and Sustainable Energy, Advanced Materials Research, Vol. 347 (Trans Tech Publications, 2012) pp. 124–127

15. N. Latip, H. Ng, N. Farah, K. Ramesh, S. Ramesh, and S. Ramesh, Organic Electronics 41, 33 (2017).

16. M. Buraidah, S. Shah, L. Teo, F. I. Chowdhury, M. Careem, I. Albinsson, B.-E. Mellander, and A. Arof, Electrochimica Acta 245, 846 (2017). [100] M. Cui and P. S. Lee, Chemistry of Materials 28, 2934 (2016).

17. Y.-J. Lee, S.-K. Jeong, and N.-J. Jo, Composite Interfaces 16, 347 (2009).

18. M. S. Su'ait, A. Ahmad, H. Hamzah, and M. Y. A. Rahman, Journal of Physics D: Applied Physics 42, 055410 (2009).

19. C.-H. Tsai, C.-Y. Lu, M.-C. Chen, T.-W. Huang, C.-C. Wu, and Y.-W. Chung, Organic Electronics 14, 3131 (2013).

20. J.-K. Kim, Y. J. Lim, H. Kim, G.-B. Cho, and Y. Kim, Energy Environ. Sci. 8, 3589 (2015).